Distributed trajectory flexibility preservation for traffic complexity mitigation

Husni Idris, Daniel Delahaye, David Wing

Eighth USA/Europe Air Traffic Management Research and Development Seminar (ATM2009)

Distributed Trajectory Flexibility Preservation for Traffic Complexity Mitigation

Husni Idris
Advanced Transportation Research and Engineering
Global Solutions, L-3 Communication
Billerica, MA USA
husni.idris@L-3com.com

Daniel Delahaye
Applied Math laboratory
Ecole Nationale de L'Aviation Civile
Toulouse, France
daniel.delahaye@recherche.enac.fr

David Wing
NASA Langley Research Center
Hampton, VA USA
david.wing@nasa.gov

***Abstract*— The growing demand for air travel is increasing the need for mitigation of air traffic congestion and complexity problems, which are already at high levels. At the same time new information and automation technologies are enabling the distribution of tasks and decisions from the service providers to the users of the air traffic system, with potential capacity and cost benefits. This distribution of tasks and decisions raises the concern that independent user actions will decrease the predictability and increase the complexity of the traffic system, hence inhibiting and possibly reversing any potential benefits. In answer to this concern, the authors propose the introduction of decision-making metrics for preserving user trajectory flexibility. The hypothesis is that such metrics will make user actions naturally mitigate traffic complexity. In this paper, the impact of using these metrics on traffic complexity is investigated. The scenarios analyzed include aircraft in en route airspace with each aircraft meeting a required time of arrival in a one-hour time horizon while mitigating the risk of loss of separation with the other aircraft, thus preserving its trajectory flexibility. The experiments showed promising results in that the individual trajectory flexibility preservation induced self-separation and self-organization effects in the overall traffic situation. The effects were quantified using traffic complexity metrics based on Lyapunov exponents and traffic proximity.**

Keywords-Trajectory planning; trajectroy flexibility; traffic complexity; adaptability; robustness; separation assurance; self separation; self organizing; distributed air traffic management

I. INTRODUCTION

The Next Generation Air Transportation System (NextGen) is expected to receive up to three times the current traffic demand by the year 2025 [1]. In order to handle this increase in air traffic, NextGen will introduce key transformations in Air Traffic Management (ATM). Three examples of the transformations are: increasing information sharing through net-enabled information access; making access to National Airspace System (NAS) resources dependent on aircraft equipage; and aircraft trajectory-based operations enabled by aircraft ability to precisely follow customized four dimensional (4D) trajectories [1]. These capabilities enable a more optimal allocation of functions among the air traffic system agents, such as shifting the ATM system towards a distributed architecture [2]. For example, NextGen is investigating delegating more responsibility for traffic separation to the pilot [2, 3] and delegating more responsibility to airline operation centers for traffic flow management [3, 4]. Enabling the gains of distributed decision making depends on the ability of distributed actions to maintain safety and efficiency at acceptable levels.

Research on distributed ATM has focused, in part, on the distribution of separation responsibility between pilots and controllers. Pilots are assisted in predicting and resolving loss of separation by cockpit automation, known generally as Airborne Separation Assistance Systems (ASAS) [5, 6]. Early ASAS experiments showed positive results of self separation operations [7, 8]. Research has also concentrated on assisting ground-based controllers with automation, such as the Center TRACON Automation System [9]. Distributed traffic flow management has been limited to the incorporation of user preferences in traffic manager decisions with recent efforts to increase user responsibility [4].

Neglecting to regulate traffic beyond the separation assurance time horizon may cause complex traffic situations to arise. Many approaches have been documented to define and measure traffic complexity, most often as a function of controller workload. These metrics are primarily based on airspace geometry such as aircraft density and mix, sector geometry, traffic flow structure, and mix of aircraft types and performance characteristics [10]. Other efforts emphasized cognitive elements of complexity, in particular the controller use of standard flows, grouping of traffic, and merge points [11]. Some metrics have been proposed that are independent of the airspace structure and controller perspective. For example,

This research was funded by NASA under contract NNA07BA86C.

Delahaye et al. [12] introduced complexity metrics based on traffic organization or disorder (topological entropy). Complex traffic situations may be difficult to control, whether by ground-based or by aircraft-based agents, leading to compromised safety. Therefore, reducing or preventing such situations is a prerequisite to enabling manageable separation assurance and safety.

In order to mitigate traffic complexity, ground and airborne systems may benefit from preserving trajectory flexibility. Trajectory flexibility preservation enables an aircraft to plan its trajectory such that it preserves a requisite level of maneuvering flexibility in order to accommodate later disturbances caused, for example, by other traffic and weather activity. The hypothesis is that if each aircraft preserves its own trajectory flexibility, using an air-based or ground-based system, acceptable traffic complexity will naturally be achieved. As discussed in [13, 14], although flexibility preservation does not explicitly coordinate between aircraft, it assists each by reducing the risk of conflict due to the potential behavior of the surrounding traffic, thus resulting in implicit coordination. This function offers a trajectory-oriented approach to managing traffic complexity, by explicitly planning aircraft trajectories, such that their contribution to complexity is minimized. This is contrasted with airspace-oriented approaches that aim to ensure that airspace characteristics (such as sector size and route patterns) and traffic characteristics (such as aircraft density) are designed to dynamically limit traffic complexity.

Flexibility preservation complements separation assurance both within the conflict resolution horizon and beyond it to an extended flexibility planning horizon. Within the conflict resolution horizon, flexibility aids in selecting conflict resolution solutions that afford the aircraft more flexibility, for example, to adapt to potential intruder behavior. Beyond the conflict resolution horizon, which is the focus of this paper, flexibility preservation plans the aircraft trajectory to minimize its exposure to disturbances such as weather cells and dense traffic. Fig. 1 depicts an example. In its upper portion each aircraft, while planning its trajectory between weather cells, questions whether it should modify its trajectory to increase flexibility. If the aircraft proceed along their depicted headings, a complex traffic situation arises causing excessive congestion and a high potential conflict rate. On the other hand, the lower portion displays a structured traffic pattern that would result if each aircraft maneuvered to increase its own flexibility.

To test this hypothesis, trajectory flexibility metrics have been defined in previous work to represent robustness and adaptability to the risk of violating separation, airspace hazards, and traffic flow management constraints [14-16]. In this paper, the impact of using these metrics on traffic complexity is analyzed. Two scenarios are analyzed in two-dimensional en route airspace, where each aircraft must meet a required time of arrival (RTA) in a one-hour time horizon using speed and heading degrees of freedom. Simultaneously, each aircraft preserves its trajectory flexibility, using the defined metrics, to mitigate the risk of loss of separation with the other aircraft. The effects were quantified using traffic complexity metrics based on Lyapunov exponents [12], flow pattern consistency, and proximity. The experiments showed promising results in terms of mitigating complexity as measured by these metrics.

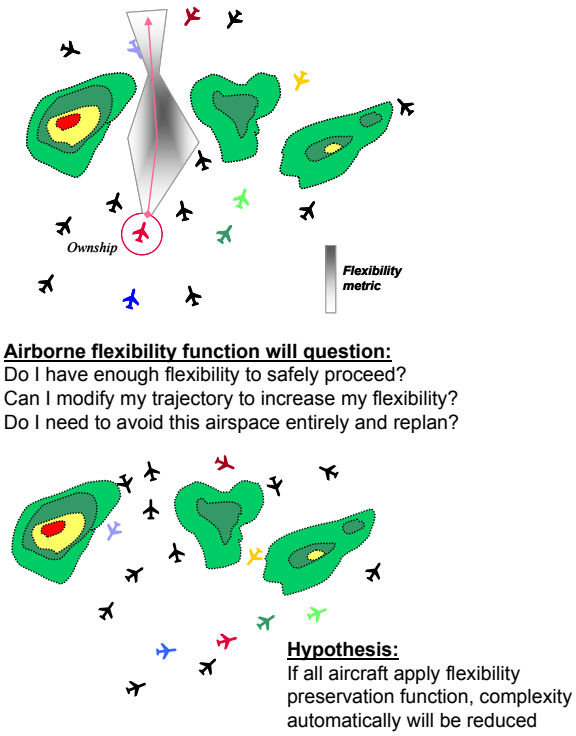

Figure 1. Trajectory Flexibility Preservation

II. METRICS

Metrics that represent trajectory flexibility have been developed and reported in previous papers [15-16] and are summarized briefly in this section. To test the hypothesis, traffic complexity metrics based on intrinsic trajectory complexity [12], traffic pattern consistency and proximity were used. These metrics are also briefly described in this section.

A. Trajectory Flexibility Metrics

The notion of "trajectory flexibility" was defined in [14] as the ability of the trajectory (and hence the aircraft following the trajectory) to abide by all constraints imposed on it while mitigating its exposure to risks that cause violation of these constraints. The constraints intend to achieve ATM and aircraft objectives and include heading limits, RTAs, and separation minima. They define the trajectory solution space. Risk of constraint violation is represented by disturbances that cause the aircraft trajectory to violate or potentially violate constraints. Disturbances were classified in [14-16] into state disturbances that result in aircraft state deviation along its trajectory or constraint disturbances such as new constraints or modifications of currently imposed or known potential constraints.

Two trajectory characteristics relevant to measuring this notion of flexibility have been identified: robustness and adaptability [14]. Metrics have been proposed for robustness and adaptability based on estimating the number of feasible trajectories available to the aircraft to accommodate

disturbances [15-16]. In order to support these definitions and estimation methods, the following assumptions are made:

(1) The aircraft is assumed to follow segments of discrete time length, where instantaneous heading and speed changes can only occur at discrete instances in time that are ε apart.

(2) Heading h and speed V take discrete values between h_{min} and h_{max} and between V_{min} and V_{max} and are constant along each segment. (Altitude is not considered in this paper.)

In addition to simplifying the estimation method, these assumptions are reasonable from an operational point of view considering the intended application of the trajectory flexibility metrics. Namely, the metrics are intended for relative comparison of trajectories over a long time horizon suitable for strategic planning (typical of traffic flow management planning horizon) as opposed to tactical maneuvering (where the dynamics of the speed and heading change are relevant).

(1) Robustness is defined as the ability of the aircraft to keep its planned trajectory unchanged in response to the occurrence of disturbances. For example, a trajectory that remains feasible in terms of meeting an RTA and maintaining separation despite the disturbances (i.e., no matter which trajectory or conflict instances materialize) is robust to these disturbances.

A robustness metric RBT(traj) is associated with a trajectory (traj) starting from a state (t, x, y) and ending at another state such as (RTA, x_{dest}, y_{dest}). RBT(traj) is measured with the probability of feasibility P_f(traj) of the trajectory, which can be estimated with partial information about state and constraint disturbances that represent the risk of constraint violation or infeasibility. Estimating P_f(traj) requires probabilistic models of the state and constraint disturbances. As an example, consider a state disturbance that makes every trajectory instance from a state (t, x, y) to the destination e.g., (RTA, x_{dest}, y_{dest}) possible with equal probability. In this case, the trajectory (traj) is modeled by N(t, x, y) instances ($traj_i$) each with equal probability

$$P_i(t,x,y) = \frac{1}{N(t,x,y)}, \text{ with } \sum_{i=1}^{i=N} P_i = 1.$$

Each constraint situation c divides the total set of trajectories N(t, x, y) into two mutually exclusive subsets: f_c(t, x, y) the set of feasible trajectories with respect to c and i_c(t, x, y) the set of infeasible trajectories with respect to c. Hence, N(t, x, y) = f_c(t, x, y) + i_c(t, x, y). Then, the following formula can be derived for robustness RBT(t, x, y); see [15, 16] for more detailed derivation:

$$P_{f,c}(t,x,y) = \frac{f_c(t,x,y)}{N(t,x,y)}$$

$$RBT(t,x,y) = P_f(t,x,y) = \sum_{c=1}^{c=C} P_c \times \frac{f_c(t,x,y)}{f_c(t,x,y) + i_c(t,x,y)} \quad (1)$$

where $P_{f,c}$ is the probability of feasibility of the trajectory traj in a constraint situation c, and is equal to the ratio of the number of feasible trajectories f_c to the total number of trajectories N. The constraints are modeled with C constraint situations c each with a probability P_c with $\sum_{c=1}^{c=C} P_c = 1$.

(2) Adaptability is defined as the ability of the aircraft to change its planned trajectory in response to the occurrence of a disturbance that renders the current planned trajectory infeasible. An adaptability metric ADP(t, x, y) is associated with a state (t, x, y) along a trajectory and is measured by the number of feasible trajectories f(t, x, y) (with respect to all constraints) that are available for the aircraft to use at (t, x, y) to regain feasibility. Then, given the probability distribution (P_c) of each constraint situation c of C, ADP may be estimated by the average over C:

$$ADP(t,x,y) = f(t,x,y) = \sum_{c=1}^{c=C} P_c \times f_c(t,x,y). \quad (2)$$

Adaptability decreases as the aircraft moves along a trajectory because the number of feasible trajectories decreases. The special case of robustness given by (1) (robustness to totally random state disturbances) increases over time because as the number of feasible trajectories (numerator) decreases the total number of trajectories (denominator) decreases more rapidly by both infeasible and feasible trajectories.

B. Traffic Complexity Metric

The impact of planning trajectories using the adaptability and robustness metrics on traffic complexity was assessed using three main indicators: an intrinsic trajectory-based complexity metric, consistency of a resulting flow pattern, and proximity between aircraft.

The intrinsic traffic complexity metric is based on the non-linear dynamic system modeling of the aircraft trajectories. This metric identifies any kind of trajectories organization in the airspace by the mean of Lyapunov exponents map computation. Based on the observations of the aircraft (positions, speed vectors and times), a non linear space-time dynamic system has to be adjusted with the minimum error.

$$\dot{\vec{X}}(t) = f(\vec{X}, t)$$
$$\min \sum_{i=1}^{i=N} \sum_{k=1}^{k=K} \left\| V_i(t_k) - f(\vec{X}_i, t_k) \right\| \quad (3)$$

where N is the number of aircraft and K the number of samples per aircraft trajectory.

There are many classical ways of obtaining a class of parametrized vector fields that fulfill the fitting requirement. Among them, vector splines allow control on the smoothness of vector fields, which is important in this case since civil aircraft maneuvers are based on low acceleration guidance laws. The vector field is designed to minimize a function form

$$\min \int_{R^4} \int_R \alpha \left\| \nabla \mathrm{div} \vec{f}(\vec{X}, t) \right\|^2 + \beta \left\| \nabla \mathrm{curl} \vec{f}(\vec{X}, t) \right\| + \left\| \frac{\partial \vec{f}(\vec{X}, t)}{\partial t} \right\| d\vec{X} dt \quad (4)$$

with α, β ,γ positive real numbers controlling the smoothness of the approximation by focusing on constant divergence or constant curl.

Computing traffic complexity for a given traffic situation requires interpolating a vector field given only samples (positions and speeds of aircraft at given times). Vector spline interpolation seeks the minimum error between the observation

and the model. This adjustment is done with a Least Square Minimization (LMS). The metric chosen for complexity computation relies on a measure of sensitivity to initial conditions of the underlying dynamic system called Lyapunov exponents. The Lyapunov exponents are closely related to the singular values of the gradient matrix on the vector field at a given point.

$$\kappa(\vec{f}) = \frac{1}{n}\sum_{i=1}^{i=n}\left\| D_{\vec{X}}\vec{f}(\phi(t,\vec{X}))\right\| 2 \qquad (5)$$

where $D_{\vec{X}}$ is the gradient matrix of the field at point $\vec{X}$ and $\phi(t,\vec{X})$ the point trajectory of the dynamic system at point $\vec{X}$.

When Lyapunov exponents are high, the trajectory of a point under the action of the dynamic system is very sensitive to the initial conditions (or parameters on which the vector field may depend), so that the situation in the future is unpredictable. On the other hand, small values of the Lyapunov exponents mean that the future is highly predictable (very organized traffic). So, the Lyapunov exponent map determines the area where the underlying dynamic system is organized. It identifies the places where the relative distances between aircraft do not change with time (low real value) and the ones where such distance changes a lot (high real value). More information about this metric may be found in [12].

Flow pattern consistency was also measured by the percentage of aircraft that followed a consistent pattern. The pattern was readily apparent visually so no clustering technique was employed in the scenarios analyzed in this paper. The pattern, as described in Section IV, was scenario dependent. Traffic proximity was measured by the number of aircraft-seconds that are less than a threshold distance apart.

III. Trajectory Generation Algorithm

A dynamic programming algorithm was used to generate an aircraft trajectory using the robustness and adaptability metrics. Because the intention of this analysis is to test a hypothesis rather than a real-time application, the dynamic programming approach was selected due to its simple formulation and despite its numerical and storage limitations. First the trajectory solution space is built as a tree of discrete states connected according to reachability by the allowable discrete speed and heading values over the discrete time increments. Second, the robustness and adaptability metrics are estimated at each state. Third and finally a back-propagation algorithm computes a cost function and builds a trajectory that optimizes the cost function.

A. Flexibility Metric Estimation

The calculation of the adaptability and robustness metrics requires estimation of the number of feasible trajectories from a state (t, x, y) to the destination (location, time, or both). A method was developed in [15] and [16] for varying speed along a fixed path and for varying heading, respectively. Here, this method is generalized to scenarios involving both speed and heading as degrees of freedom in situations involving RTA and separation constraints, under the two simplifying assumptions of discrete time, heading and speed, described in Section A.

Under these assumptions, the number of trajectories may be estimated using a convolution and filtering technique. Fig. 2 demonstrates this method for calculating $f_c(t, x, y)$ from any point (t, x, y) to a destination specified by a point (RTA, x_{dest}, y_{dest}) and a tolerance circle around it in the x-y plane, in a constraint situation c that includes an instance of a potential conflict. The three-dimensional space is discretized into time steps ε-apart, where in each time step, the x-y plane is discretized into square cells. The function $f_c(t, x, y)$ is estimated for each cell. Assume the function $f_c(t_j, x, y)$ at time t_j is known. The function $f_c(t_{j-1}, x, y)$ at the previous time step t_{j-1} can be obtained by convoluting $f_c(t_j, x, y)$ and the function $g_k(x, y)$, which represents the number of trajectories that reach from a point k=(t_{j-1}, x(k), y(k)) at time step t_{j-1} to the next time step t_j. The function g is independent of time. There is one trajectory that reaches from point k at step t_{j-1} to each of a set of discrete locations at step t_j – each corresponds to one pair of discrete heading and speed values. Therefore, the reachability function $g_k(x, y)$ which is shown as a conical shell in Fig. 2 is given by:

$$\begin{aligned} g_k(x,y) = 1 \;:(t_j, x, y) \in \\ \{(t_j, x(k) + V_{min}\cos(h_{min})\varepsilon, y(k) + V_{min}\sin(h_{min})\varepsilon), \cdots, \\ (t_j, x(k) + V_i\cos(h_i)\varepsilon, y(k) + V_i\sin(h_i)\varepsilon), \cdots, \\ (t_j, x(k) + V_{max}\cos(h_{max})\varepsilon, y(k) + V_{max}\sin(h_{max})\varepsilon)\} \\ g_k(x,y) = 0 \qquad \text{elsewhere} \end{aligned} \qquad (6)$$

The convolution operation amounts to calculating $f_c(t_{j-1}, x(k), y(k))$ at point k, by multiplying the values of $f_c(t_j, x, y)$ by the number of trajectories that reach from point k to (t_j, x, y) and adding them, and then repeating the operation for each point k in the x-y plane at time step t_{j-1}. However, if the point k is infeasible (for example due to loss of separation) then $f_c(t_{j-1}, x(k), y(k)) = 0$. This requires a filtering step before each convolution operation to zero out the values at infeasible states. Substituting a dummy variable τ to denote sliding the point k in the x-y plane, the function $f_c(t_{j-1}, x, y)$ is given by the following equation, representing convolution and filtering for infeasibility:

$$\begin{aligned} f_c(t_{j-1}, x, y) &= \sum_{\lambda}\sum_{\tau} f_c(t_j, \tau, \lambda) g(x - \tau, y - \lambda) \quad \text{if feasible} \\ f_c(t_{j-1}, x, y) &= 0 \qquad\qquad\qquad\qquad\quad \text{if infeasible} \end{aligned} \qquad (7)$$

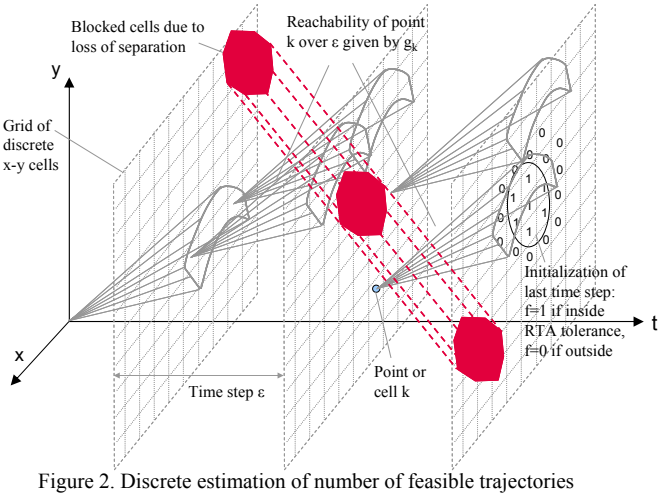

Figure 2. Discrete estimation of number of feasible trajectories

This operation is applied starting from the destination step t = RTA and proceeding backwards to the current state. The destination time step is initialized by setting $f_c(RTA, x, y) = 1$ at the feasible states and zero elsewhere as shown in Fig. 2.

To compute the total number of trajectories, N(t, x, y) used in the denominator of the robustness metric RBT, certain constraints are excluded from the filtering process (namely the constraints with respect to which robustness is computed). In this paper robustness only to loss of separation with traffic and hazards is considered. Therefore, the numerator filtering was applied to all cells that lead to separation loss as well as cells that lead to violating speed and heading limits or violating the RTA constraint. On the other hand filtering ignored loss of separation but was applied to the RTA and heading and speed limit constraints for calculating the denominator.

Separation zones were modeled as circles with given radii surrounding each intruder aircraft trajectory. Because a trajectory consists of discrete segments, each with constant speed and heading, the circle moves with constant speed and heading for the duration of each segment. In each segment, the circle is enclosed with eight tangent planes, each two opposing tangents resulting from a combination of heading and speed limits of the ownship aircraft relative to the intruder (There are four such combinations). A cell loses (or is imminent to lose) separation if it falls on the inside of all eight planes, within the time duration of the segment. The intersection of these planes with the solution space blocks polygon areas in the x-y grids, as shown in Fig. 2 for one segment. Hazards are similarly modeled as circles with zero speed. Therefore, the hazard circle is enclosed with four tangent planes rather than eight.

Under probabilistic models of disturbances, the estimation process is repeated for each constraint situation c. Then, the estimates $f_c(t, x, y)$ are averaged over all situations C to obtain the adaptability or robustness metrics (1) and (2). The convolution operation produces an exponential growth of the number of feasible trajectories $f_c(t, x, y)$ backwards with time, depicting the decrease of adaptability with time. The infeasible regions eliminate trajectories as the function $f_c(t, x, y)$ is zeroed at these states. This produces troughs or valleys in the function $f_c(t, x, y)$ depicting the impact of constraints. These are shown in Fig. 3 and 4 for an analysis case.

B. Cost Function and Trajectory Building

Given the structure of the solution space, dynamic programming offers a straightforward method to build an optimal trajectory. Using recursive back-propagation and starting from the final time step, the minimum cost of proceeding from each cell to the destination is computed and stored. This minimum cost Q(t, x(k), y(k)) for each cell k is computed by minimizing, over its reachable cells given by $\{(t+1, x, y) : g_k(t+1, x, y) = 1\}$ in the next time step t+1, the sum of the minimum cost Q(t+1, x, y) already computed for each of the reachable cells (t+1, x, y) plus the cost of proceeding from k to that cell, given for short by $q(k \rightarrow (t+1, x, y))$. A generic formula is:

$$Q(t,x(k),y(k)) = \min_{x,y:\, g_k(t+1,x,y)=1} \{Q(t+1,x,y) + q(k \rightarrow (t+1,x,y)\} \quad (8)$$

Four functions for the local cost, q, were used in the experiments reported in this paper. A function representing minimal path length was used as a baseline. Functions representing maximizing adaptability, maximizing robustness, and maximizing both combined with minimizing path length:

$$q(k \rightarrow (t+1,x,y)) = \text{distance}(k \rightarrow (t+1,x,y)) = \text{dist} \quad (9)$$

$$q(k \rightarrow (t+1,x,y)) = -\text{ADP}(k) \quad (10)$$

$$q(k \rightarrow (t+1,x,y)) = -\text{RBT}(k) \quad (11)$$

$$q(k \rightarrow (t+1,x,y)) = -\text{ADP}(k) - a^T \text{RBT}(k) + b^T \text{dist} \quad (12)$$

where a and b are weights that trade robustness and distance, respectively, with adaptability. They are raised to the power of time T (measured from the final time step) to account for the exponential growth of ADP. Note that while the accumulated distance over time is minimized, ADP and RBT are maximized at each time step (because their accumulation at any point is identical over all trajectories to the destination).

After storing the optimal costs for each cell, a forward loop builds a trajectory by tracing the optimal cells starting from the initial state. Any ties between cells were broken randomly.

IV. Complexity Impact Analysis

The estimation technique and trajectory optimization algorithm were implemented in a MATLAB tool. The resulting trajectories were analyzed using the traffic complexity metrics described in Section III B. First the two scenarios reported in this paper are described. Second, observations are made on the impact of trajectory planning, using the four cost functions (9) through (12), on traffic complexity.

A. Analysis Scenarios

The first of two scenarios consists of a line of weather cells leaving two holes for which two flows of traffic compete. The two traffic flows travel in opposite directions: one starts at x = 0, y = −120 nautical miles and heads towards x = 0, y = 80 nautical miles. The other flow starts at x = 0, y = 120 and ends at x = 0, y = −80 nautical miles. Five weather hazard cells are modeled as circles with a radius of 20 nautical miles, and located at x = 0 and y = {0, ±70, ±120 nautical miles} as shown in Fig. 5. The geometry of the hazards and of the traffic start and end positions is selected to provide symmetry, such that the path length alone is not a differentiator for selecting among the two holes. This ensures highlighting the impact of the robustness and adaptability metrics compared to shortest path. Each traffic flow is generated with random entry times separated by intervals between five and seven minutes. All aircraft are limited to headings of ±60 degrees relative to the centerline connecting the start and end positions, with 10-degree increments. They are also limited to a speed between 240 and 360 knots with 10-knot increments. Each aircraft is assigned an RTA at the destination that forces the aircraft to path stretch to meet the RTA. This was ensured by setting the RTA up to 10 minutes above the travel time at minimum speed along a straight path. The RTA is met exactly with no tolerance at the destination point allowed.

The second scenario consists of a weather cell that causes four traffic flows crossing at right angles to go around the

weather cell in a round about. The weather cell is modeled as a circle with radius of 30 nautical miles located at (x = 0, y = 0). The four traffic flows originate at (x = 0, y = −120), (x = 0, y = 120), (x = −120, y = 0) and (x = 120, y = 0). They end respectively at (x = 0, y = 80), (x = 0, y = −80), (x = 80, y = 0) and (x = −80, y = 0). All units are in nautical miles. Eight other hazard circles are added at the corners as shown in Fig. 6 (discussed in Section B) to increase the traffic interaction around the hazard located in the center. The speed and heading limits and increments are the same as in the first scenario. The entry times for each flow ranged between 6 and 8 minutes.

In both scenarios, each aircraft plans a trajectory to meet the RTA (using speed reduction and path stretching), optimizing the four cost functions (9) through (12). Time increments of 2 minutes and square x-y cells of 2 nautical miles are used in the estimation of the number of trajectories. The first aircraft does not encounter any traffic as it plans its trajectory. Then, each following aircraft plans its trajectory assuming knowledge of the trajectories of all preceding aircraft. These trajectories are surrounded by separation zones that, in addition to the weather hazards, are avoided by the aircraft. Hazards and separation zones reduce the number of feasible trajectories. Therefore, earlier aircraft are given priority while each later aircraft encounters exceedingly more traffic. No dynamic trajectory modification is considered in the experiments run for this analysis. Each aircraft generates one trajectory upon its entry and maintains this trajectory throughout. Also the experiment runs considered only deterministic aircraft behavior. One trajectory is considered for each aircraft with probability of one. However, the separation requirement around each aircraft was set to 10 nautical miles (instead of the required 5 nautical miles) in order to capture the higher uncertainty in the rather long time horizon of these experiments. Fig. 3 shows an example of the adaptability metric (ADP) at one time step of the solution space, for an aircraft that encounters the hazards of the first scenario. Color shades are used to depict the log of the number of feasible trajectories. Fig. 4 shows an example of the robustness metric (RBT) at one time step of the solution space using color shades. Note that adaptability is highest near the center of the solution space around the central hazard, while robustness is highest near the extremities of the solution space away from the central hazard. Also note that robustness here is with respect to the hazards and loss of separation only and not to the RTA constraint or the speed and heading limits. Finally it should be noted that the solution space is smaller in Fig. 4 because it is an earlier time step and that these figures are in a relative frame with respect to an aircraft (hence the hazard y-location is 120 nautical miles rather than zero).

Each scenario contained 80 aircraft distributed evenly among the flows. The resulting trajectories consist of heading and speed decisions at each two-minute increment. They are then interpolated with 30 second time steps assuming constant speed and heading in each two-minute time increment. Finally they are analyzed for traffic complexity.

B. Results and Observations

Fig. 5 (a-e) demonstrates the resulting flow patterns in the first scenario and Fig. 6 (a-e) those in the second scenario,

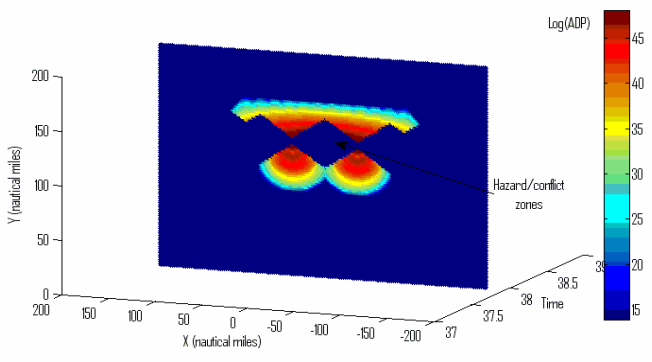

Figure 3. Example of adaptability metric map

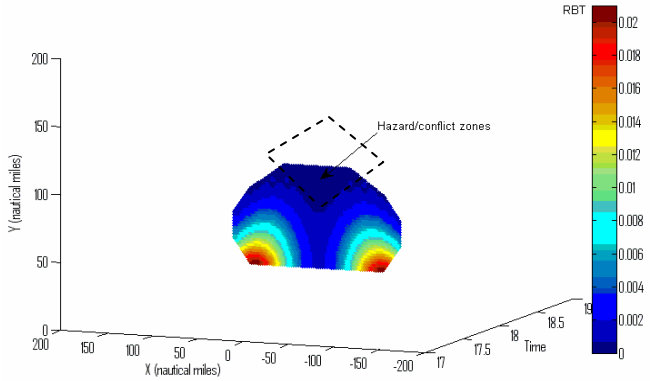

Figure 4. Example of robustness metric map

using an eight-minute time history. As a baseline, the shortest path cost function (9) was run twice, once without avoiding the other traffic (case a) and once with avoiding it (case b). Traffic avoidance was turned off to depict current practice where conflict avoidance is only applied in a short time horizon of 10 to 20 minutes. Shortest-path with traffic avoidance sets another baseline for demonstrating the marginal effect of using the adaptability and robustness metrics in cases c-e. When using the adaptability and robustness metrics (cases c-e) traffic is naturally avoided because the number of trajectories at cells that lose separation is zero. However, avoiding loss of separation is not guaranteed because of the coarse discretization of the solution space. The larger the time and space increments, the larger the chance of losing separation.

Traffic complexity was measured using the metric given by (3)-(5). The resulting complexity maps (Lyapunov exponents) are shown as background to the traffic scenarios in Fig. 5 and 6. The maps in Fig. 5 were derived using a twelve-minute window and the ones in Fig. 6 using a three-minute window (the twelve-minute average did not highlight enough details in this case). The Lyapunov exponent maps demonstrate the predictability of the flow in the snap shots used in these figures. Note that the color scale is unique for each of the cases, but the numbers on the scale can be compared between cases. The high numbers indicate less predictability and hence less organized traffic areas as discussed in Section III.B.

Fig. 5 and 6 demonstrate that, in both scenarios, using robustness and adaptability as objectives for individual trajectory planning resulted in more structured aggregate traffic

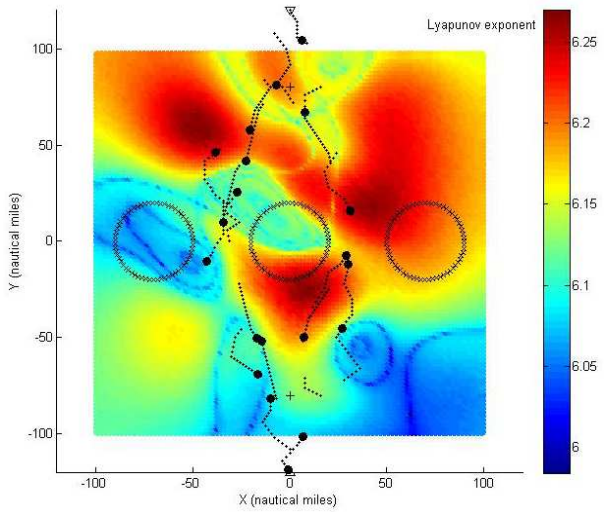

(a) Shortest path without traffic avoidance
No specific pattern.

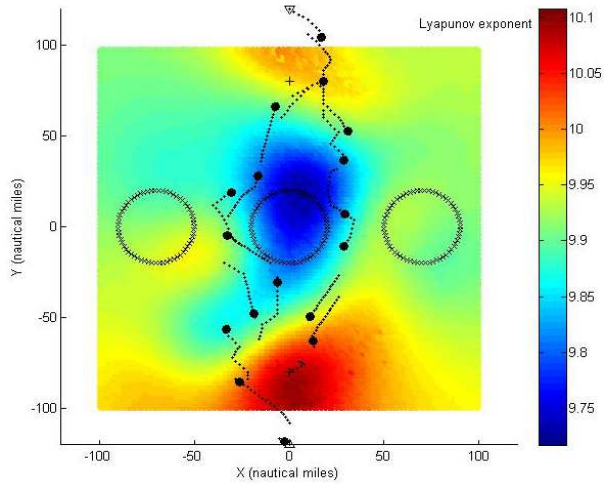

(b) Shortest path with traffic avoidance
Pattern: northbound mostly through left hole, southbound mostly through right hole

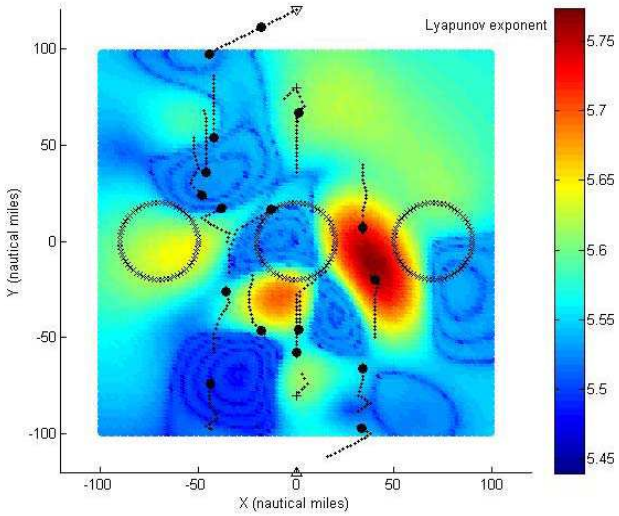

(c) Maximum adaptability only
Pattern: outer lanes before hole, along centerline after the hole

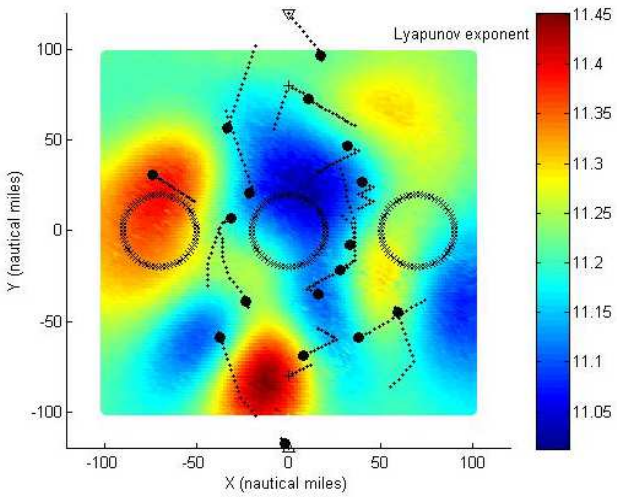

(d) Maximum robustness only
Pattern: spread out as possible

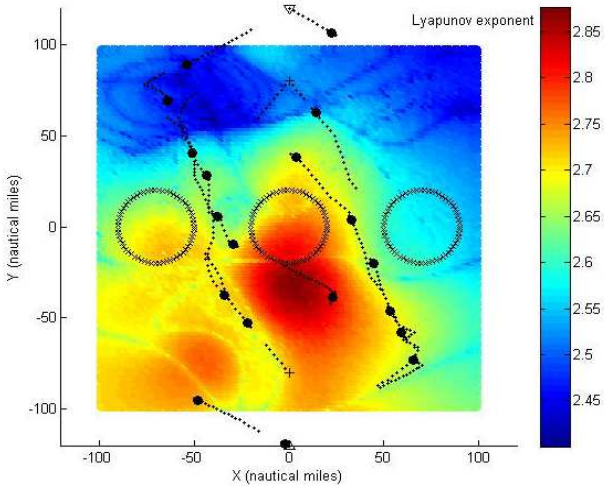

(e) Maximum adaptability and robustness, and shortest path
Pattern: mostly northbound through right hole, southbound through left hole

Figure 5. Flow patterns in weather line scenario

flow. Looking at the headings of the aircraft, shown by a black circle at the end of the eight minute history trail, and at the complexity maps, one can see the following. In case a, which used shortest path without traffic avoidance, aircraft varied in selecting their path relative to the hazard in both scenarios resulting in closer proximity and more random flow patterns. This is captured by a wide and unorganized spread of high-Lyapunov-exponent areas in case a of both figures.

All the other cases resulted in a more structured traffic pattern but in a different manner: In case b of Fig. 5, which used shortest path but avoided traffic, most aircraft traveled through the holes in a uniform direction, with occasional misalignment. In case c of Fig. 5, which used adaptability, aircraft formed outer lanes before the hazard and traveled along the centerline afterwards. This pattern resulted because adaptability tended to concentrate the aircraft trajectory close to the centerline connecting the initial and final locations. This is because the number of feasible trajectories is highest near the centerline (as shown in Fig. 3) which caused the aircraft to hug

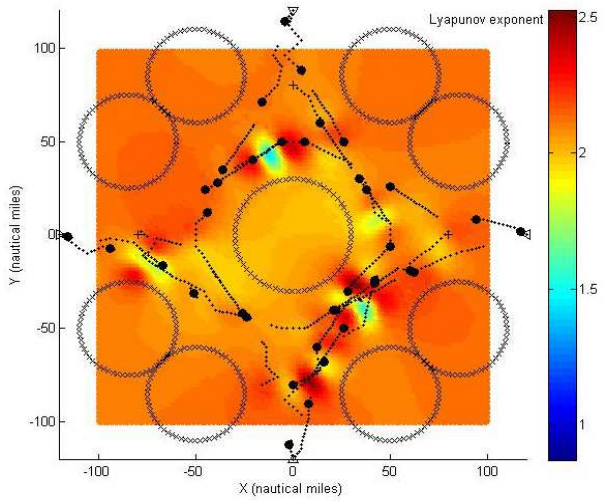

(a) Shortest path without traffic avoidance
No pattern: 60% of aircraft counterclockwise

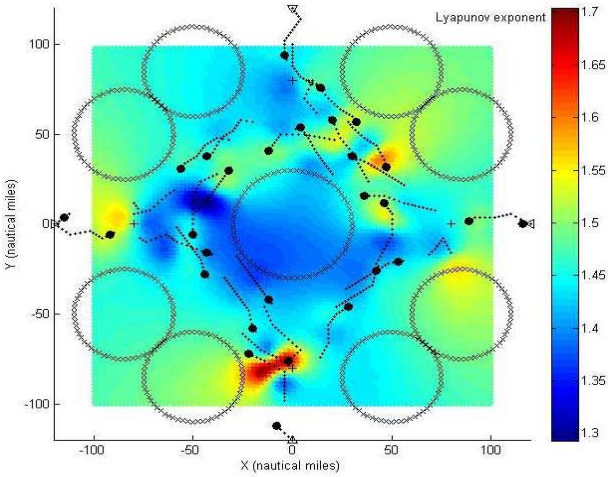

(b) Shortest path with traffic avoidance
Pattern: 68% of aircraft counterclockwise

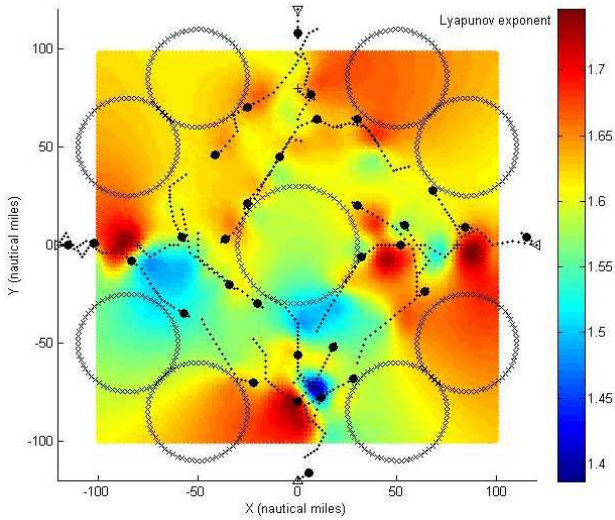

(c) Maximum adaptability only
Pattern: 97% of aircraft counterclockwise

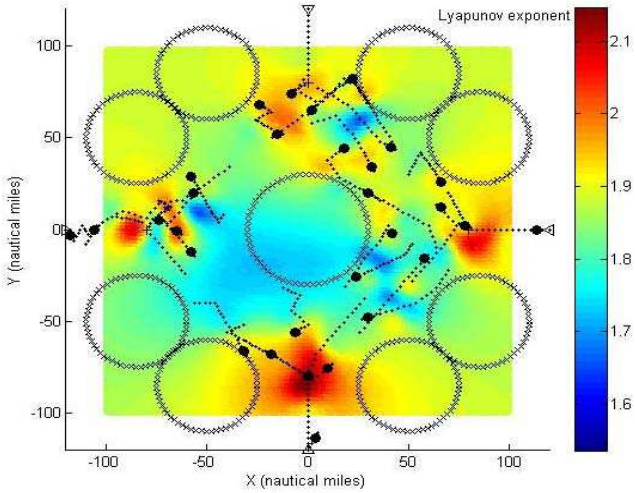

(d) Maximum robustness only
Pattern: 70% of aircraft counterclockwise

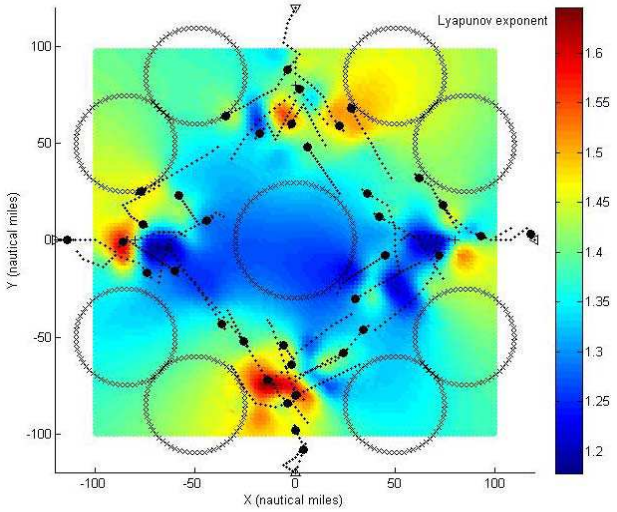

(e) Maximum adaptability and robustness, and shortest path
Pattern: 84% of aircraft counterclockwise

Figure 6. Flow patterns in round about scenario

to central hazard. The holes in this scenario were large enough to allow the aircraft to travel through them in both directions. This caused locally high Lyuaponov exponents as shown in the right hole of Fig. 5 c. On the other hand, robustness, which was used in case d, tended to send the aircraft away from each other and from the hazards increasing the spacing between them. This caused aircraft in case d to spread out more than in cases b and c, and to exhibit a less structured manner. This was also captured by areas of low predictability around strayed aircraft in Fig. 5 d. Aircraft in both cases c and d separated from each other more than in cases a and b. In case e, the aircraft formed a unidirectional flow through each of the holes. One can see in Fig. 5 e the valleys (low exponent values) along this unidirectional flow through the holes. Aircraft that did not follow this pattern are surrounded with high exponent areas.

In the round about scenario of Fig. 6, most aircraft turned around the central hazard in a uniform direction relative to the shortest path case a. This is indicated in the figure by the percentage of aircraft that selected the counterclockwise direction. This percentage is higher in cases c-e (70-97 percent)

than cases a and b (60-68 percent). The Lyapunov exponent again captures this effect. Case a in Fig. 6 has high exponent areas concentrated around the central hazard where aircraft paths cross each other randomly without avoidance. In cases b through e, the high exponent values are concentrated near the sources and destinations while the movement areas around the central hazard are relatively more organized and predictable.

In Fig. 5 and 6 cases c and d exhibited the lowest Lyapunov exponent values compared to the other cases, reflecting more organized and predictable patterns for one time step. Fig. 7 shows the average Lyapunov exponents for a series of maps over time for the scenario of Fig. 6. This average value represents the minimum information (in the Shannon sense) that has to be brought to the system in order to fully organize the traffic (with the same speed in the same direction). Fig. 7 shows that case a has the highest average value most of the time. This is consistent with the lack of organization relative to the other cases. On the other hand, case c has the lowest average most of the time also consistent with the most structured flow pattern indicated in Fig. 6. The corresponding plot for the scenario in Fig. 5 did not show such a consistent difference in the average Lyapunov exponent between the cases. This may be attributed to the fact that the patterns in this scenario were less structured over the full map area and dominated by local misalignments.

The manner and degree to which the traffic self organizes depends on a number of factors. For example, the following additional observations are made: (1) cases e of Fig. 5 and 6 combine shortest path, adaptability and robustness in the cost function (12), with a = 40 and b = 5000. These cases exhibited aspects from each of the b, c, and d cases: Because of robustness, aircraft spread out more. Because of adaptability, they formed a lane closer to the centerline especially after the hazard. Because of minimizing distance trajectories are smoother. The weights used in this example were not optimized and the tradeoff between these factors is a subject of further research. (2) The density of the traffic, a function of both the arrival rate and the size of the hazards, affects the pattern. For example, the aircraft managed to go through the holes in Fig. 5 in both directions, which caused high complexity areas captured well by the Lyapunov exponents in Fig. 5 case c. (3) The first aircraft in the scenario does not encounter any traffic and hence makes random decisions if there are ties between trajectories. The emerging pattern of the traffic depends on these early decisions. For the same reason, when the traffic density declines the pattern may switch to a new one. (4) All aircraft in these scenarios used the same objective function. This induces implicit coordination and rules and influences the emerging pattern. (5) The shortest path case, with traffic avoidance (b) is closer to the adaptability case (c) than the robustness case (d). This is because the shortest path is close to the centerline where adaptability is high. The shortest path trajectory, however, differs from the most adaptable trajectory because it uses the minimum speed (to minimize path stretching). Therefore these trajectories were smother and exhibited less turns. Adaptable trajectories on the other hand tended to zigzag around the centerline.

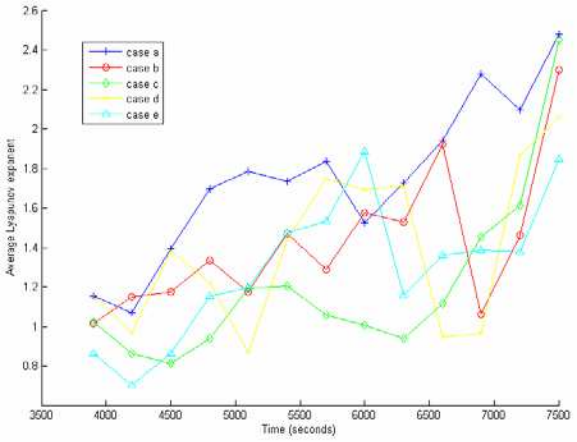

Figure 7. Average Lyapunov exponent for scenario of Fig 6

The resulting aircraft trajectories were also analyzed for proximity. Fig. 8 (a and b) display, respectively for the two scenarios of Fig. 5 and 6, the number of aircraft-seconds when aircraft were less than 20 nautical miles apart, over the duration of each scenario. These figures show that, as expected, for both scenarios the case (a) where aircraft used shortest path without traffic avoidance exhibited the highest rate of close proximity. In the first scenario (the two-hole scenario of Fig. 5) the shortest path with traffic avoidance (case b) exhibited significantly higher proximity than the other cases (c-e) that used adaptability and/or robustness. This suggests that, at least in this scenario, the use of adaptability and/or robustness metrics increases the separation between aircraft over simple traffic avoidance. However, this was not apparent in the second scenario (the round about scenario of Fig. 6) where all cases that avoided traffic (b-e) exhibited similar proximity.

V. Conclusions and Future Research

The analysis reported in this paper demonstrated that using adaptability and robustness metrics in planning flexible aircraft trajectories results in traffic complexity mitigation. Two scenarios showed signs of self separation and self organization when using these metrics. The impact was quantified using both a Lyapunov-exponent-based traffic complexity metric and a proximity rate measurement. These flexibility metrics can be combined with other metrics in the trajectory planning of pilots, airlines, and traffic managers. By incorporating these metrics, the contribution of each aircraft to traffic complexity would be reduced, even without explicit coordination among aircraft or for the aircraft by a ground system.

The results reported in this paper are promising, and open the door for a wide range of future research. Such research extension includes the investigation of: the sensitivity to varying a number of factors such as traffic density and severity of constraints; the effect of dynamic and stochastic decision making where each aircraft updates its trajectory plan over time in response to uncertainty; sensitivity to varying the cost function and the tradeoff between adaptability, robustness and other metrics of interest to users and traffic managers; the effect of non-uniform, competing cost functions among different aircraft; the impact of explicit rules and coordination on furthering self organization; and the practical application of the metrics and algorithms presented in real-time systems.

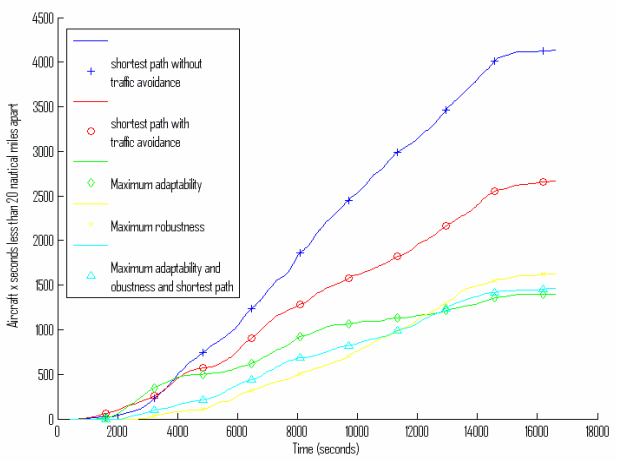

(a) Traffic complexity for the first scenario (two holes)

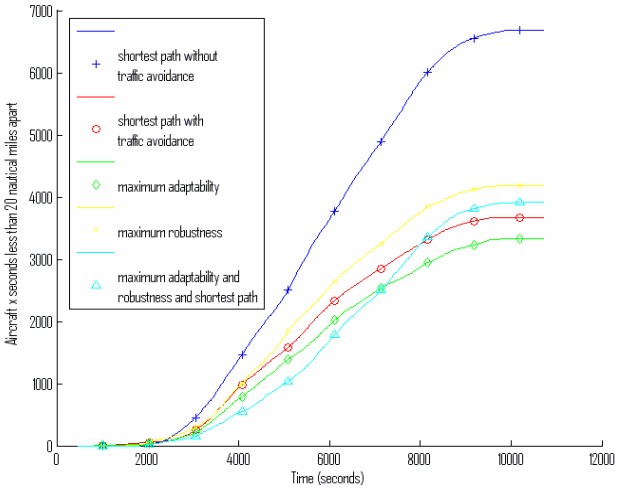

(b) Traffic complexity for the second scenario (round about)

Figure 8. Traffic proximity for the two scenarios

ACKNOWLEDGMENT

The authors would like to thank Dr. Danette Allen of NASA Langley for her valuable reviews and her support of this research and Mr. Robert Vivona and Tarek El-Wakil of L-3 Communications for valuable contributions.

REFERENCES

[1] Joint Planning and Development Office, "Next Generation Air Transportation System Integrated Plan," URL: http://www.jpdo.gov/library/NGATS_v1_1204r.pdf

[2] D. Wing, "A potentially useful role for airborne separation in 4D-trajectory ATM operations," Proceedings of the 5th AIAA Aviation Technology Integration and Operations (ATIO) Conference, AIAA-2005-7336, 2005.

[3] S. M. Green, K. D. Bilimoria, and M. G. Ballin, "Distributed air/ground traffic management for en route flight operations." Air Traffic Control Quarterly, Vol. 9, No. 4, 2001, pp. 259–285.

[4] H. Idris, R. Vivona, S. Penny, J. Krozel, and K. Bilimoria, "Operational concept for collaborative traffic flow management based on field observations," Proceedings of the 5th AIAA 5th Aviation Technology, Integration and Operations (ATIO) Conference, AIAA-2005-7434, 2005.

[5] K. Krishnamurthy, B. Barmore, and F. Bussink, "Airborne precision spacing in merging terminal arrival routes," 6th USA/Europe Air Traffic Management R&D Seminar, 2005.

[6] H. A. P. Blom, B. Klein Obbink, and G. I. Bakker, "Safety risk simulation of an airborne self separation concept of operation," Proceedings of the 7th AIAA Aviation Technology Integration and Operations (ATIO) Conference, AIAA 2007-7729.

[7] R. Barhydt, and P. Kopardekar, "Joint NASA Ames/Langley experimental evaluation of integrated air/ground operations for en route free maneuvering," 6th USA/Europe Air Traffic Management R&D Seminar, 2005.

[8] MFFP Mediterranean Free Flight Programme Final Report 2005, D821, http://www.medff.it/public/index.asp

[9] H. Erzberger, T. J. Davis, and S. M. Green, "Design of center-TRACON automation system," AGARD Meeting on Machine Intelligence in ATM, Berlin, Germany, 1993

[10] P. Kopardekar. and S. Magyarits, "Measurements and prediction of dynamic density," 5th USA/Europe ATM R&D Seminar, 2003

[11] J. Davison, J. Histon, M. Ragnarsdottir, L. Major, and R. J. Hansman, "Impact of operating context on the use of structure in air traffic controller cognitive processes". 5th USA/Europe Air Traffic Management R&D Seminar, 2002.

[12] D. Delahaye, S. Puechmorel, R. J. Hansman, and J. Histon, "Air traffic complexity based on non linear dynamical systems", 5th USA/Europe Air Traffic Management R&D Seminar, 2003.

[13] H. Idris, D. Wing, R. Vivona, and J. L. Garcia-Chico, "A distributed trajectory-oriented approach to managing traffic complexity," Proceedings of the 7th AIAA Aviation Technology Integration and Operations (ATIO) Conference, AIAA-2007-7731, 2007.

[14] H. Idris, R. Vivona, J. L. Garcia-Chico, and D. Wing, "Distributed traffic complexity management by preserving trajectory flexibility," Proceeding of the 26th Digital Avionics Systems Conference, 2007.

[15] H. Idris, T. El-Wakil, and D. Wing, "Trajectory planning by preserving flexibility: metrics and analysis," Proceedings of the AIAA Guidance Navigation and Control (GNC) Conference, AIAA-2008-7406, 2008.

[16] H. Idris, R. Vivona, and D. Wing, "Metrics for traffic complexity management in self-separation operations," ATCQ, in-press.

BIOGRAPHIES

Husni Idris received a bachelor of science (1989) and a master of science (1992) in mechanical engineering, a master of science in operations research (2000) and a Ph.D. in human factors and automation (2000), all from the Massachusetts Institute of Technology, Cambridge, Massachusetts, USA. He is a Principal Researcher in the Advanced Transportation Research and Engineering department of Global Solutions, a division of L-3 Communications. His research has focused on modeling and analysis of future ATM concepts. His domain included airport surface operations, collaborative and distributed traffic flow management, and trajectory planning.

Daniel Delahaye is working as a researcher in the applied Mathematics Laboratory of ENAC (French Civil Aviation Engineer School). He obtained his engineering degree from the ENAC school and a master of science in signal processing from the National Polytechnic Institute of Toulouse in 1991. He obtained his PH.D in automatic control from the Aeronautic and Space National school in 1995 and did a post-doc at the Department of Aeronautics and Astronautics at MIT in 1996. He conducts research on stochastic mathematical optimization. He applied his work to airspace design, traffic assignment and trajectories complexity metric.

David J. Wing holds a bachelor of science degree in mechanical engineering, Washington University, St. Louis, Missouri, USA, 1988, and a master of science degree in aeronautical engineering, The George Washington University, Joint Institute for the Advancement of Flight Sciences, Hampton, Virginia, USA, 1990. He is a Principal Researcher of ATM at the NASA Langley Research Center in Hampton, Virginia, USA. He specializes in developing and investigating ATM operational concepts that involve airborne separation and airborne trajectory management. He has conducted several piloted simulation studies of autonomous aircraft operations and technology and is author on over 20 publications on these and related topics.